RSC Advances

ROYAL SOCIETY OF CHEMISTRY

www.rsc.org/advances

A comparative study of the molecular structure, lipophilicity, solubility, acidity, absorption and polar surface area of coumarinic anticoagulants and direct thrombin inhibitors

Milan Remko*, Ria Broer, Anna Remková

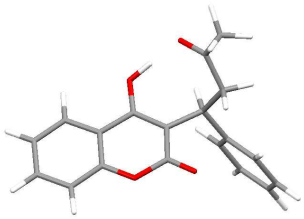

WARFARIN

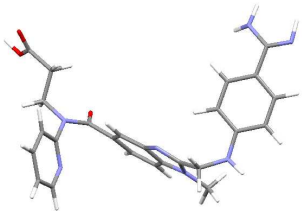

DABIGATRAN

The methods of computational chemistry have been used to elucidate the molecular properties of coumarinic anticoagulants (acenocoumarol, phenprocoumon, warfarin and tecarfarin) and direct thrombin inhibitors (melagatran, dabigatran and their prodrug forms, ximelagatran and dabigatran etexilate).

A comparative study of the molecular structure, lipophilicity, solubility, acidity, absorption and polar surface area of coumarinic anticoagulants and direct thrombin inhibitors

Milan Remko[a,b,*], Ria Broer[c], Anna Remková[b],

[a]*Comenius University in Bratislava, Faculty of Pharmacy, Department of Pharmaceutical Chemistry, Odbojarov 10, SK-832 32 Bratislava, Slovakia*
[b]*Center for Hemostasis and Thrombosis, Hemo Medika Bratislava, Šustekova 2, 851 04 Bratislava, Slovakia*
[c]*Department of Theoretical Chemistry, Zernike Institute for Advanced Materials, University of Groningen, Nijenborgh 4, 9747 AG Groningen, The Netherlands*

Abstract

The methods of computational chemistry have been used to elucidate the molecular properties of coumarinic anticoagulants (acenocoumarol, phenprocoumon, warfarin and tecarfarin) and direct thrombin inhibitors (melagatran, dabigatran and their prodrug forms, ximelagatran and dabigatran etexilate). The geometries and energies of these drugs have been computed at the Becke3LYP/6–311++G(d, p) level of theory. In the case of the vitamin K antagonists (acenocoumarol, phenprocoumon, warfarin and tecarfarin), the most stable tautomer in both the gas-phase and water solution is tautomer A, which contains the 4-hydroxycoumarin moiety. The *R*(+)-enantiomer of this tautomer is the most stable structure in warfarin and acetocoumarol. For phenprocoumon, the *S*(–) enantiomer was the most stable species. The computed dissociation constants show that these drugs are almost completely ionized at physiological p*H* = 7.4. Tecarfarin is the vitamin K antagonist with the highest lipophilicity. The prodrugs ximelagatran and dabigatran etexilate are described as lipophilic drugs. The prodrugs' metabolites, melagatran and dabigatran, are substantially less liphophilic. The relatively high polar surface area value of acenocoumarol (113.3) results in lessened absorption in comparison with warfarin. Phenprocoumon, with PSA value 50.4, had the highest calculated absorption of all of the anticoagulants in the study. The direct thrombin inhibitors, melagatran and dabigatran, have a high total number of proton donor and proton acceptor groups (15), a high PSA (150) and the lowest absorption of the drugs studied.

Keywords: vitamin K antagonists; direct inhibitors of thrombin; molecular structure; solvent effect; pK_a; lipophilicity, solubility, absorption and polar surface area

1. Introduction

Coagulation (thrombogenesis) is characterized by the formation of a blood clot in a blood vessel, leading to series of complications, such as atrial fibrillation (AF), artificial heart valves, deep vein thrombosis (DVT), pulmonary embolism (PE), stroke and heart attack[1,2]. Anticoagulants are key drugs that reduce the body's ability to form blood clots[3-8]. Parenterally administered unfractionated heparin and orally administered vitamin K antagonists (warfarin) have been the main drugs of anticoagulant therapy for decades[8,9]. However, such problems as the need for frequent dose adjustment and monitoring of coagulation status, as well as multiple drug and food interactions (warfarin), make the use of vitamin K antagonists unappealing for both physician and patient[10,11]. There is a growing interest in new, orally active anticoagulants with significant advantages over current agents, such as heparin and warfarin, for the treatment and prevention of thrombotic diseases. Recently, new direct thrombin inhibitors and direct factor Xa (fXa) inhibitors have been introduced into clinical use for venous thromboembolism treatment[4-8,10-13]. The thrombin inhibitors melagatran and dabigatran block the activity of thrombin, the enzyme that catalyzes the conversion of fibrinogen to fibrin[5,12].

Numerous direct, selective factor Xa inhibitors are currently at various stages of development in different therapeutic indications[4,5]. Small-molecule synthetic compounds, such as rivaroxaban, apixaban and edoxaban, are members of a new class of orally available active-site-directed factor Xa inhibitors[6,13,14]. Despite considerable experimental evidence for the relationship between the chemical and pharmaceutical properties of coumarinic anticoagulants, their structural and pharmacokinetic parameters are not very well understood. Valente et al. determined the crystal structure of *S*(–)-warfarin[15]. The molecule crystallized as the structurally modified intramolecular hemiketal[15], one of the several possible tautomers of warfarin[16]. However, the 4-hydroxycoumarin tautomer of the warfarin moiety is present in the crystal structure of warfarin sodium 2-propanol solvate[17]. The mechanism of conversion between the major isomeric forms of warfarin has been studied theoretically[18]. Kostova et al. investigated the experimental and theoretical spectra of warfarin sodium[19] and acenocoumarol[20]. Porter recently reviewed the history of investigations on the tautomerism of warfarin in relation to its pharmaceutical and chemical properties[21]. Karlson et al.[22] investigated the role of the structural diversity of warfarin on its distribution in a model phospholipid bilayer membrane. The direct inhibitors of thrombin dabigatran and dabigatran etexilate have been studied theoretically[23]. Shen et al. reported the crystal structure of dabigatran

etexilate tetrahydrate[24]. Despite extensive pharmacological investigation of direct antagonists of vitamin K and newer drugs targeting thrombin, there is no single experimental study concerned with the systematic comparative investigation of the physicochemical and pharmacokinetic parameters of these medicinally useful oral anticoagulants.

In this study, we use several computational chemistry methods to study the molecular structure, pK_a, lipophilicity, solubility, absorption and polar surface area of coumarinic anticoagulants (acenocoumarol, phenprocoumon, warfarin and tecarfarin) and direct thrombin inhibitors (melagatran, dabigatran and their prodrug forms). The results of our studies of these drugs were compared with the available experimental data and discussed in relation to the present theories of action of these agents. In the absence of large-scale experimental data, our theoretical results may enhance the understanding of the subtle biological effects of these anticoagulants with regard to comparisons of "classical" warfarin-like drugs and new oral anticoagulant drugs and thrombin inhibitors.

2. Computational Details

Theoretical calculations of the coumarinic anticoagulants (acenocoumarol, phenprocoumon, warfarin and tecarfarin) and direct thrombin inhibitors (melagatran, dabigatran and their prodrug forms) (Fig. 1) were conducted with the Gaussian 09 computer code[25] at the density functional theory (DFT, Becke3LYP[26-28]) level of theory using the 6–311++G(d, p) basis set[29]. To evaluate the conformational behavior of these systems in solvent, we performed optimization calculations in the presence of water. For the estimation of the hydration free energy, we applied the polarizable continuum method using the conductor-like polarizable continuum model (CPCM)[30-33]. The structures of all gas-phase species were fully optimized at the B3LYP/6–311++G(d, p) levels of theory without any geometrical constraint. The lipophilicity and water solubility calculations were performed using web-based VCCLAB[34,35]. Calculations of the macroscopic pK_a values were performed using the program SPARC[36]. The computer program SPARC, developed by Carreira et al.[37,38], uses computational algorithms based on fundamental chemical structure theory to estimate a variety of chemical reactivity parameters (such as ionization pK_a, kinetics, heat of vaporization, boiling point and diffusion coefficient). SPARC costs the user only several minutes of computer time and provides greater accuracy than is possible with other conventional methods[39]. For

calculations of the molecular polar surface areas, the fragment-based method of Ertl and coworkers,[40,41] incorporated in the Molinspiration Cheminformatics software,[42] was used.

3. Results and Discussion

3.1. Molecular structures

All of the coumarinic anticoagulants studied possess the same 3-benzyl-hydroxycoumarin functionality. The relative orientation of the functional groups in the coumarinic anticoagulants (defined by the dihedral angles α, β, γ, δ, ε and ζ) is shown in Fig. 1. The important geometrical parameters (dihedral angles) describing the relative molecular orientation of the drugs studied are given in Tables 1 and 2. An analysis of the harmonic vibrational frequencies of the optimized species revealed that all the structures obtained were minima (no imaginary frequencies). Acenocoumarol, phenprocoumon and warfarin are chiral molecules and are administered as racemates and, based on their different metabolism, exhibit differences in pharmacokinetic and pharmacodynamic properties.[3,43] Warfarin is almost completely (approximately 99%) bound to human serum albumin (HSA), the major component of blood plasma[44]. The crystal structures of HSA-myristate complexed with the *R*(+)- and *S*(–)-enantiomers of warfarin have shown that the two enantiomers of this drug adopt notably similar conformations when bound to the HSA[45,46]. However, under different chemical environments, warfarin may undergo a series of isomerization reactions[21]. In our work, the *S*(–)- and *R(+)*-enantiomers of warfarin itself were considered in two enol tautomeric forms (**A** and **B**) and a hemiketal form (**C**), as seen in Fig. 1. The intramolecular hemiketal structure of warfarin is observed experimentally[12] in the solid state. However, the conformation of warfarin bound at the transport protein HSA is either the *S*(–)-enantiomer (pdb code 1HA2) or the *R*(+)-enantiomer (pdb codes 2BXD and 1H9Z) of the open side chain deprotonated state of tautomer **A**.[44,45]

The relative orientation of the anticoagulant moiety of the direct inhibitors of thrombin, defined by individual dihedral angles (α, β, γ, δ, ε, ζ, η, and θ, Fig. 1), was taken from the experimental X-ray data of the crystal structures, deposited in the Protein Data Bank[46] (PDB), of the complex of the ethylester of dabigatran with thrombin (PDB: 1HTS), the complex of the melagatran with thrombin (PDB: 1K1P, 4BAH) and the X-ray structure of the dabigatran etexilate tetrahydrate[24]. The important dihedral angles of melagatran, dabigatran and their prodrugs ximelagatran and dabigatran etexilate together with the available X-ray structures of these drugs in

the unbound and/or bound state (at the receptor), are given in Table 3. The overall shape of the most stable species is presented in Fig. 1A of the electronic Supporting Material. Values for the dihedral angles for the individual thrombin inhibitors are different (Table 3), and no general conclusions about the pharmacophore functionality can be deduced. Experimentally, small molecule drug conformations are commonly studied using X-ray crystallography. In the absence of published experimental X-ray structural data for melagatran and dabigatran, quantum chemistry methods present a challenge to obtain information about the stable conformations of these drugs in the gas phase and in solution. A comparison of the *ab initio* SCF calculated conformational energies of drug molecules with the conformer distribution in the solid state routinely exhibit a good correlation[47]. For the comparison and analysis of the theoretically determined conformations and protein-bound conformations of the thrombin inhibitors, we also present the available structural data for bound anticoagulants on the thrombin receptor. Table 4 contains the total and relative energies of the coumarinic anticoagulants studied (Fig. 1). The B3LYP-optimized, most stable conformers of these coumarinic anticoagulants are shown in Fig. 1A of the supplementary material. The hydration free energies computed using the CPCM method are presented in Table 5. It has been shown previously[48] that the conductor-like polarizable method reproduces hydration energies with an accuracy on the order of a few kcal/mol but usually (70% of the cases) better than one kcal/mol. The anticoagulant drugs exhibit the greatest stability in solvent, as expected, because they contain considerable dipole moments (Table 5). Water has a remarkable effect on the energy and geometry of the anticoagulants studied. The energy difference between the gas phase and solvated phase is always negative; larger stabilization energies were computed for sodiated drugs. We also carried out quantum chemical calculations to discuss the tautomers of coumarinic anticoagulants and clarify their relative stability depending on chemical environments. In the gas phase and aqueous solution, we discussed the dominant forms in tautomers of warfarin, acenocoumarol, phenprocoumon and tecarfarin, respectively (Table 4). Focusing on the solvent effect, the conductor-like polarizable continuum model (CPCM) has been used in this study. This model allows one to take into account long-range interactions and allows the molecular geometry and dipole moment of the solute to be adjusted to reflect the interaction of the aqueous solution. Although continuum CPCM model used in this work does not account specific hydrogen bonding effects on the tautomerism, it is simple to implement and is computationally efficient for the prediction of general structural and stability trends in aqueous phase.

Warfarin and warfarin sodium

The dosage of warfarin (3-(alpha-acetonylbenzyl)-4-hydroxycoumarin) is a racemate, with *S*(–)-warfarin being three times as potent as *R*(+)-warfarin[3]. However, from a clinical standpoint, *R*(+)-warfarin is the most active anticoagulant because CYP2C9 metabolizes *S*(–)-warfarin in the first-pass-effect very efficiently[3]. The *R*(+)-enantiomer of tautomer **A** has the lowest energy (Table 4). In the solid state, the most stable hemiketal, tautomer **C,** of this enantiomer is the second most stable species with an energy difference of 8.79 kJ/mol. A different situation exists with the 2-hydroxysubstituted tautomer **B** of *S*(–)-warfarin. The most stable species of this tautomer is the hemiketal form **C** and is, in comparison with the absolute minimum tautomer, less stable by 14.32 kJ/mol (Table 4). The solvent effect further lowered the relative stability of the individual species studied, and the hemiketal isomer **C** of *R*(+)-warfarin may coexist with its open chain form **A**. The third most stable tautomer (the hemiketal form of *S*(–)-warfarin) is approximately 6.7 kJ/mol less stable. The calculated population ratios in water solution for these three stable species at 310.2 K are 72 : 23 : 5. The **A** tautomer of *R*(+)-warfarin is stabilized in the gas phase via an intramolecular hydrogen bond of the O–H···O=C type with a computed distance 1.82 Å, which is less than the sum of the van der Waals radii[49] of hydrogen and oxygen atoms (2.7 Å). This intramolecular hydrogen bond is also preserved in water solution (a value of 1.746 Å was computed for the O(5)–H···O=C separation of the solvated tautomer). This H-bond is also responsible for the displacement of the OH hydrogen atom (by approximately 30^{o}) out of the plane of C(3)-C(4)-O(5) heavy atoms, dihedral angle ε (Table 1). In the absence of intramolecular stabilization, the hydroxy group is oriented almost coplanar to the coumarin moiety. The optimal dihedral angles of the warfarin species with the CPCM method and solvent water are different. The difference in dihedral angles α[C(2)-C(3)-C(7)-C(8)] and β[C(3)-C(7)-C(8)-C(9)] can be as large as 20^{o} in some tautomers (Table 1).

The conformation of a drug bound to the protein differs from that of an unbound molecule in the crystal structure and also from the most thermodynamically stable structure of the isolated molecule[50]. Although the quality of ligands within published X-ray structures of protein–ligand complexes is, in many cases, rather poor[51], we also compared the conformations of bound and unbound warfarin. The superimposition of the 3-D structures of the *R*(+)- and *S*(–)-warfarin complexed with the HSA-myristate and the isolated species is shown in Fig. 2. Conformations of bound and unbound warfarin differ in the mutual position of alpha-acetonylbenzyl moiety (dihedral angles α[C(2)-C(3)-C(7)-C(8)], γ[C(3)-C(7)-C(10)-C(11)] and δ[C(7)-C(10)-C(11)-O(12)]). The conformation of bound warfarin, although determined at lower level of resolution[45] (2.5 Å),

indicates that the geometry of warfarin in its HSA-myristate complex is far different from the conformation of the isolated molecule (Fig. 2). However, the superimposition of the X-ay molecular structures of the *R*(+)- and *S*(–)-warfarin bound to human serum albumin (Fig. 2A of the Supplementary material) shows that the coumarinic and aromatic moieties of both enantiomers occupy almost the same space. The main conformational difference is observed for the acetonyl group, and the dihedral angles γ[C(3)-C(7)-C(10)-C(11)] and δ[C(7)-C(10)-C(11)-O(12)] for the individual enantiomers are considerably different (Table 1).

The most stable structures of warfarin sodium in the gas phase and water solution correspond to tautomer A of the *R*(+)-warfarin. The Na^+ cation is almost symmetrically coordinated to oxygen atoms O(5) and O(12) (Fig. 1A of the Supporting Material). This sodium bond is also responsible for the displacement of the O···Na moiety out of the plane of the C(3)-C(4)-O(5) heavy atoms with a dihedral angle ε [C(3)-C(4)-O(5)-Na] –58.5^o (Table 1). The second most stable tautomer (29.7 kJ/mol less stable) is tautomer **A** of the *S*(–) enantiomer. The sodium cation in this tautomer is coordinated to the O(5) oxygen atom with the equilibrium O(5)···Na^+ distance equal to 2.099 Å and strong $Na^+ – \pi$ interaction with phenyl moiety (Fig. 1A of the Supporting Material). The stabilization effect of the alkali metal cation – π interactions between the alkali metals and the aromatic side chains of the aromatic amino acids is also observed in metallic complexes of these amino acids[52]. The sodium cation in tautomer B of both enantiomers of warfarin sodium is bicoordinated to the O(1) and O(6) oxygen atoms of the coumarin moiety (the distances Na^+···O(1) and Na^+···O(6) are approximately 2.30 Å and 2.15 Å, respectively. Microsolvation results in considerable prolongation of the Na^+···O(1) and Na^+···O(6) distances by approximately 0.2 – 0.4 Å.

Acenocoumarol

The B3LYP total and relative energies of the four calculated species of acenocoumarol (4-hydroxy-3-[1-(4-nitrophenyl)-3-oxobutyl]-2H-chromen-2-one) are listed in Table 4. Both the *R*(+)- and *S*(–) enantiomers of acenocoumarol are pharmacologically active[43] as antagonists of vitamin K, although the *R* enantiomer was reported to be several times more potent than the *S* enanthiomer[53]. The acenocoumarol was considered in two sets (tautomers **A** and **B**) of individual enantiomers (Fig. 1). Tautomer A of the *R*(+)-acenocoumarol is the most stable species in both vacuum and water solution (Table 4). The conformation of *R*(+)-acenocoumarol is, as in warfarin, stabilized via an intramolecular hydrogen bond of the O(5)-H···O=C type. A value of 1.806 Å was calculated for the

r(O(5)-H···O) separation. The importance of this intramolecular hydrogen bond for the stabilization of the gas-phase structure of warfarin is also manifested the appreciable deviation of the 4-OH group from planarity. The most important is the non-planar conformation around the C(4)–O(5) bond displacing the O(5)-H hydrogen atom out of the coumarin-ring plane by approximately 30^{o} (dihedral angle ε[C(3)-C(4)-O(5)-H], Table 2). In the absence of this intramolecular hydrogen bond, the acetonyl and benzyl groups of *R*(+)-acenocoumarol are more severely rotated out of the plane of the coumarin-ring plane (dihedral angle α[C(2)-C(3)-C(7)-C(8)], Table 2). In the absence of conformational stabilization of the alpha-acetonylbenzyl moiety via intramolecular hydrogen bonding O-H···O=C in the **A** and **B** tautomers of *S*(–)-acenocoumarol, the molecular conformation of these two tautomers of *S*(–) enantiomer is similar. In water solution, the most appreciable conformational changes (approximately 5 – 15^{o}) in all investigated species of acenocoumarol are related to the conformation around the C(7)–C(8) bond of the benzyl group (dihedral angle β[C(3)-C(7)-C(8)-C(9)]).

Phenprocoumon

Phenprocoumon (3-(alpha-ethylbenzyl)-4-hydroxycoumarin) is a chiral drug. The *S*(–)-enantiomer is predominantly responsible for the anticoagulant effects of phenprocoumon[3]. Theoretical calculations of the total and relative energies of the fully optimized four principal species of both enantiomers studied have shown that in contrast with warfarin and acenocoumarol, the most stable species is tautomer **A** of *S*(–)-phenprocoumon (Table 4). For enhanced stability of this tautomer in both vacuum and water solution, the favorable interaction of a polar hydroxyl group O(5)-H with the π-system of the benzyl ring is responsible (Fig. 1A of the Supplementary material). The stabilizing effect of the O(5)-H···π interaction is also observed with tautomer **A** of *R(+)*-phenprocoumon. However, this tautomer is 22.2 kJ/mol less stable (Table 4). A molecular superimposition of the **A** tautomer of both enantiomers (Fig. 3) indicates that the benzyl ring is oriented differently (torsion angles α[C(2)-C(3)-C(7)-C(8)] and β[C(3)-C(7)-C(8)-C(9)]) and the O(5)-H group is rotated out of the coumarin plane by approximately 10 – 15^{o}. Appreciable changes of these dihedral angles are observed in water solution (Table 2).

Tecarfarin and tecarfarin sodium

Tecarfarin (4-(4-hydroxy-2-oxo-2H-chromen-3-ylmethyl)-benzoic acid 2,2,2-trifluoro-1-methyl-1-trifluoromethyl-ethyl ester) is a drug candidate that is in clinical trials[54,55]. Compared to warfarin, it has decreased potential to interact metabolically with drugs that inhibit CYP450 enzymes and therefore may offer an improved safety profile for patients[55]. Both tecarfarin and its sodium salt may exist in two tautomeric forms, **A** and **B** (Fig. 1). According to our calculations, tautomer **A** is the only stable form of tecarfarin in the gas-phase and solvated state (Table 4). In this tautomer, the polar hydroxyl group O(5)-H interacts with the π-system of benzoic acid (Fig. 1A of the Supplementary material). In the sodium salt, the difference between the two tautomers is small (17.56 kJ/mol), and in water solution, both species may coexist with calculated population ratios for these two stable tautomers at 310.2 K of 84 : 16. The sodium cation is always bicoordinated. Whereas in tautomer **A,** coordination of Na^+ occurs between the O(5) oxygen atom and the π-system of aromatic ring of benzoic acid substituents, for tautomer B, the bifurcate bond O(1)···Na^+···O(6) is characteristic (Fig. 1A of the Supplementary material). Solvation is connected with high changes of equilibrium geometry, especially in sodiated tecarfarin (dihedral angles β[C(3)-C(7)-C(8)-C(9)] and ε[C(3)-C(4)-O(5)-Na] change upon hydration by approximately 30 – 40^o)

Melagatran and ximelagatran

Melagatran (N-((R)-(((2S)-2-((-p-amidobenzyl)carbamoyl)-1-azetidinyl)carbonyl)cyclohexyl–methyl)glycine), the active metabolite of prodrug ximelagatran (ethyl 2-{[(1R)-1-cyclohexyl-2-[(2S)-2-[({4-[(Z)-N'-hydroxycarbamimidoyl]phenyl}methyl)carbamoyl]azetidin-1-yl]-2-oxoethyl]amino}acetate) was the first oral direct thrombin inhibitor approved for clinical use; however, high hepatotoxicity led to the forced withdrawal of this drug from the market in February 2006[14]. The important geometrical parameters are given in Table 3. Several trends are apparent: the optimized geometries of both ximelagatran and its active metabolite melagatran occupy the same space and manifested corresponding dihedral angles (Table 3). In both molecules, the most stable structures are the conformers possessing the characteristic L-shaped conformation stabilized by means of the intramolecular hydrogen bond N(10)–H···O=C(6) with a length of 1.97 Å for both molecules. The amidine group of the benzimido residue is rotated out of the aromatic ring plane by approximately 25^o (dihedral angle θ[C(14)-C(15)-C(16)]-N(17)]). The solvent effect results in only a slight structural rearrangement (Fig. 3A of the Supplementary Material). The overall conformation

of the benzimido residue and the p-amidobenzyl moiety is preserved in the biologically active conformation of melagatran bound at the thrombin binding site (torsion angles ζ, η, and θ, Table 3). However, the overall geometry of the biologically active conformation of melagatran is different (Fig. 4A of the Supplementary material), and upon complexation with thrombin, large changes of dihedral angles α, β, γ, δ, and ε were observed (Table 3).

Dabigatran and Dabigatran Etexilate.

Dabigatran (3-[[2-[[(4-carbamimidoylphenyl)amino]methyl]-1-methylbenzimidazole-5-carbonyl]-pyridin-2-ylamino]propanoic acid) is a direct inhibitor of thrombin that binds to thrombin with high affinity and specificity. Because dabigatran is not orally active in clinical praxis, it is used in the form of a double prodrug, dabigatran etexilate (ethyl-3-[[2-[[[4-(N'-hexoxycarbonylcarbamimidoyl) phenyl]amino]methyl]-1-methylbenzimidazole-5-carbonyl]-pyridin-2-ylamino]propanoate)[56,57]. The molecular structure of these drugs analyzed in our previous paper[23] using the double-ζ basis set 6–31++g(d, p). An extension of the basis set to the triple-ζ quality 6–311++G(d, p) resulted in minimal changes in the computed equilibrium geometry of the isolated molecules (Table 3). Table 3 contains selected X-ray data for dabigatran etexilate tetrahydrate[24]. The solid state structure of the tetrahydrated complex of dabigatran etexilate differs considerably from the optimized molecule in the gas phase or hydrated state. The main difference between the gas–phase and solid-state structures arises from the fact that the molecular conformation of dabigatran etexilate in the solid state is affected by crystal packing forces and solvated water molecules forming a layer of a tetrameric hydrogen bonding network via the intermolecular hydrogen bonds O–H···O, O–H···N and N–H···O strongly coordinated to the dabigatran etexilate (Fig. 1A of the Supplementary material). The optimal geometry of dabigatran and dabigatran etexilate computed using the CPCM method do not considerably differ in water solution from those obtained for the isolated molecules (Table 3).

3.2. Dissociation constants

Dissociation plays important part in both the partition and the process of the binding of studied anticoagulants with their receptor. Coumarinic anticoagulants contain an acidic functionality (a hydroxyl group) that can be 4-hydroxy (tautomer **A**) and/or 2-hydroxy (tautomer **B**); thus, they may undergo a dissociation reaction. The ionization state of this group plays an important role in

determining the physicochemical properties of these drugs. We applied the p*K*a predictor implemented in the program SPARC[36] to compute the theoretical p*K*a values of the studied anticoagulants in the condensed phase (water). Table 6 contains the calculated macroscopic p*K*a values of the studied drugs. The acidity of the two main tautomers, **A** and **B,** of the coumarinic drugs (acenocoumarol, phenprocoumon, warfarin) is slightly different, and at physiological p*H* = 7.4 they are almost completely ionized. The experimental p*K*a value of 5.06 for warfarin was also reported[58]. A slightly higher p*K*a value of 5.15 was measured by Porter[21]. The hemiketal structure of warfarin had no ionizable site in the normal p*K*a range (Table 6). Tecarfarin's calculated p*K*a values for the **A** and **B** tautomers are different and low, and this drug is almost fully ionized at physiological pH (Table 6). There is experimental evidence that the biologically active forms of the coumarinic anticoagulants studied is anionic with the negative charge localized on the oxygen attached to C(4) of the coumarin moiety[21,59]. Melagatran and dabigatran possess both acidic and basic functionality. Both groups are at ionized at blood pH and exist as zwitterionic structures[60].

3.3 Lipophilicity and solubility

Drug lipophilicity and solubility are important descriptors governing permeation across a biological membrane[61]. It is therefore important to determine these physicochemical properties associated with a drug before synthetic work is begun. Lipophilicity is expressed quantitatively as log*P* and is the most widely used predictor for drug permeation. However, log*P* does not encompass the extent of ionization of ionizable molecules. For drugs that have ionizable groups, the distribution coefficient (log*D*), which considers the extent of ionization as well as the intrinsic lipophilicity, may be a better descriptor for the partitioning of a mixture of drug species as well as the actual drug lipophilicty at any given pH[62]. The computed log*P* values (*P* is the partition coefficient of the molecule in a water – octanol system) and the available log*D* values, together with the experimental data, are shown in Table 7. The ALOGPS method[63-65] is used to predict the lipophilicity and the aqueous solubility of compounds. The lipophilicity calculations within this method are based on the associative neural network approach and the efficient partition algorithm. The LogKow (KowWIN) program[66] estimates the log octanol/water partition coefficient (log*P*) of organic chemicals and drugs using an atom/fragment contribution method developed at Syracuse Research Corporation[67]. The XLOGP3 is an atom-additive method that applies corrections[68,69]. Experimental log*P* values of acenocoumarol, phenprocoumon, warfarin and dabigatran etexilate were extracted from the literature[70]. Whereas the

biological properties of the chiral anticoagulants acenocoumarol, phenprocoumon and warfarin vary[3], many of the physicochemical properties of their enantiomers must be identical[71]. Lipophilicity and solubility are achiral descriptors and should be the same for the *S*(−) and *R*(+) enantiomers. In the case of tautomers, due to their unique 3D structure, various species may also exhibit different physical properties. With regard to lipophilicity, the atom additive XLOGP3 method is unable to discriminate between the **A** and **B** tautomers of acenocoumarol, phenprocoumon and warfarin (Table 7). The computed partition coefficients (ALOGPS method) for the drugs studied varied between −0.5 and 5.2. Tecarfarin is the vitamin K antagonist with the highest lipophilicity. The variation in the lipophilicity of the series of vitamin K antagonists is high and spans an interval of approximately 2 log*P* units (Table 7).

The prodrugs ximelagatran and dabigatran etexilate are described as lipophilic drugs. The prodrugs' metabolites, melagatran and dabigatran, are substantially less liphophilic (Table 7). Melagatran is a highly hydrophilic drug with a computed negative log*P* value and poor lipid bilayer permeability. Melagatran interacts with human α-thrombin via an extensive network of hydrogen bonds[72.] Conversely, the binding of the more hydrophobic dabigatran to the thrombin active site results, apart from the salt bridge with Asp 189, results solely from hydrophobic interactions[73].

The anticoagulants studied are almost completely ionized at p*H* = 7.4 (Table 6). For ionizable drugs, the effective lipophilicity is pH-dependent, and the distribution coefficient log*D* will be different from log*P*. The log*D* values, calculated from the predicted log*P* (ALOGP method) and p*Ka* (Sparc) using the equation[74] $\log D = \log P - \log (1+10^{pH\text{-}pKa})$ for acids, are presented in Table 7. The calculated $\log D_{7.4}$ values for the vitamin K antagonists are substantially lower. The predicted $\log D_{7.4} = 0.67$ for the warfarin **A** tautomer fits well with the experimentally determined[75] value of 0.78.

Log*S,* the intrinsic solubility in the neutral state, is indicative of a compound's solubility (S). The log*S* values were calculated using the web-based VCCLAB ALOGPS predictor (Table 7). The experimentally determined solubilities of phenprocoumon (12.9 mg/L), warfarin (17 mg/L) and dabigatran etexilate (1.8 mg/L) closely matched the calculated values (Table 7). Drug solubility is one of the important factors that affects the movement of a drug from the site of administration into the blood. Insufficient solubility of drugs can lead to poor absorption[76]. Investigation of the rate-limiting steps of human oral absorption of 238 drugs (including warfarin) has indicated[76] that the absorption of a drug is usually very low if the calculated solubility is < 0.0001 mg/L. The anticoagulants studied are only slightly soluble in water; their computed solubilities between 2 and

120 mg/L are sufficient for fast absorption. Coumarinic anticoagulants in the free-acid form are not very soluble in water and are therefore administered in the form of their sodium salts. The highest solubility of approximately 100 mg/L was predicted for the highly polar direct thrombin inhibitors melagatran and dabigatran. These drugs contain a benzamidine and a carboxylate group and in aqueous solution exhibit amphoteric properties. Because of their highly polar, zwitterionic nature, and a log$D_{7.4}$ = –3.79 and –0.79, they have no appreciable bio-availability after oral administration.

3.4. Absorption, polar surface area, and "rule of five" properties

High oral bioavailability is an important factor for the development of bioactive molecules as therapeutic agents. Important predictors[77,78] of good oral bioavailability include passive intestinal absorption, reduced molecular flexibility (measured by the number of rotatable bonds), low polar surface area and total hydrogen bond count (sum of donors and acceptors). Properties of molecules, such as bioavailability or membrane permeability, have often been connected to simple molecular descriptors such as log*P*, molecular weight (*MW*), or counts of hydrogen bond acceptors and donors in a molecule[79]. Lipinski[80] used these molecular properties in formulating his "Rule of Five". The guidelines based on Lipinski's work state that most orally active molecules with good membrane permeability have logP ≤ 5, molecular weight ≤ 500, number of hydrogen bond acceptors ≤ 10, and number of hydrogen bond donors ≤ 5. This guideline is widely used as a filter for drug-like properties. Table 8 contains the calculated percentages of absorption (%ABS), molecular polar surface areas (PSA) and Lipinski parameters of the anticoagulants investigated. The magnitude of absorption is expressed by the percentage of absorption. Absorption percent was calculated[76] using the expression: %ABS = 109 – 0.345 PSA. The polar surface area (PSA) was determined by the fragment-based method of Ertl and coworkers[40,41]. The relatively low number of rotatable bonds in acenocoumarol, phenprocoumon and warfarin indicates that these ligands, upon binding to receptor, change their conformation only slightly. Tecarfarin contains more rotatable bonds (7), which impart some flexibility on the non-pharmacophoric structural unit-ester moiety. A relatively high value of polar surface area of acenocoumarol (113.3) results in reduced absorption in comparison with warfarin (Table 8). Phenprocoumon, with PSA value 50.4, was the anticoagulant with the highest calculated absorption.

Melagatran, the first oral direct thrombin inhibitor approved for clinical use, violated the "rule of five" (too many proton donors). This drug's double prodrug, ximelagatran, obeys this rule. However, because of high hepatotoxicity, this drug was withdrawn from the market in 2006. The prodrug dabigatran etexilate violated "rule of five" (too high molecular weight); however, its noticeably increased lipophilicity (approximately 2 – 2.5 log*P* units, Table 7) compared to dabigatran enabled oral administration of this drug. The direct thrombin inhibitors melagatran and dabigatran are very flexible molecules with high total numbers of proton donor and proton acceptor groups (15), high PSA (approximately 150) and lowest absorption of the compounds studied (Table 8). Due to poor adsorption, dabigatran has only low bioavailability[1] (7%); therefore, to reach adequate plasma levels, a relatively high oral dose is needed. At physiological conditions, melagatran and dabigatran are present in the form of charged species. The ionization of acidic or basic groups and the high PSA of these drugs are not compatible with their oral application. Oral administration is enabled through their double prodrugs eliminating charges and thus increasing the lipophilicity of the molecule (Table 7).

4. Conclusions

This theoretical study set out to determine the stable conformations, solvent effect, acidity, lipophilicity, solubility, absorption and polar surface area of vitamin K antagonists (acenocoumarol, phenprocoumon, warfarin and tecarfarin) and direct thrombin inhibitors (melagatran, dabigatran and their prodrug forms ximelagatran and dabigatran etexilate), for which a relatively small amount of experimental physicochemical data exists, considering their pharmacological importance. Using theoretical methods, the following conclusions can be drawn.

i) In the case of the coumarinic anticoagulants, the fully optimized most stable forms are the 4-hydroxycoumarin **A** tautomers. In the case of chiral anticoagulants, the *R*(+)-enantiomer of this tautomer is the most stable structure in warfarin and acetocoumarol. However, for phenprocoumon, the most stable form is the *S*(–) enantiomer. This stability order correlates with the anticoagulant response of chiral vitamin K antagonists. For the overall anticoagulant response, the *R*(+)-warfarin, *R*(+)-acenocoumarol and *S*(–)-phenprocoumon are responsible.[2]

ii) Water has a strong effect on the geometry of the anticoagulants studied. The energy difference between the gas phase and the solvated phase is always negative, and larger stabilization energies were computed for the sodiated drugs.

iii) Coumarinic anticoagulants contain an acidic functionality (a hydroxyl group), which may be the 4-hydroxy (tautomer **A**) and/or the 2-hydroxy (tautomer **B**), and thus, they may undergo a dissociation reaction. The acidity of these two tautomers is slightly different, and at physiological pH = 7.4, they are almost completely ionized. Melagatran and dabigatran possess both acidic and basic functionality. Both groups are ionized at blood pH and exist as zwitterionic structures.

iv) The computed partition coefficients (ALOGPS method) for the drugs studied varied between –0.5 and 5.2. Tecarfarin is the vitamin K antagonist with the highest lipophilicity. The variation in the lipophilicity of the series of vitamin K antagonists is high and spans an interval of approximately 2 log$P$ units. The prodrugs ximelagatran and dabigatran etexilate are described as very lipophilic drugs. For ionizable drugs, the effective lipophilicity (the distribution coefficient log$D$) was also evaluated.

v) The anticoagulants studied are only slightly soluble in water; their computed solubilities from 2 to 120 mg/L are sufficient for fast absorption. Coumarinic anticoagulants in the free acid form are not very soluble in water and are therefore administered in the form of their sodium salts.

vi) A relatively high value of polar surface area of acenocoumarol (113.3) results in reduced absorption compared to warfarin. Phenprocoumon, with PSA value 50.4, was the anticoagulant with the highest calculated absorption. The direct thrombin inhibitors melagatran and dabigatran are very flexible molecules with a high total number of proton donor and proton acceptor groups (15), high PSA (150) and the lowest absorption of the anticoagulants studied.

This work yields quantities that may be inaccessible by or complementary to experiments and represents the first theoretical approach in which a comparative study of molecular structure, lipophilicity, solubility, acidity, absorption and polar surface area of vitamin K antagonists and direct thrombin inhibitors was accomplished. Such investigations may be, due to the present recognition of the important potential commercial value of the accurate prediction of physicochemical and pharmacokinetic factors for the designing of highly effective ligands, useful in the design of new drugs for the prevention and treatment of a broad variety of conditions, including the prevention of venous thromboembolism, manifesting as deep-vein thrombosis or pulmonary embolism in patients undergoing major orthopedic or general surgery, acutely ill nonsurgical patients and cancer patients. These ligands may exhibit improved properties and intellectual property value.

Acknowledgement

This work has been supported by The European Union HPC-Europa Transnational Access Program under the Project HPC-Europa2 (Project No 863) at SARA Amsterdam. The authors acknowledge with thanks the Stichting Academisch Rekencentrum Amsterdam (SARA) for the use of its resources and for excellent support. M.R. thanks the Department of Theoretical Chemistry, Zernike Institute for Advanced Materials, University of Groningen, for its hospitality during his study stay in Groningen.

References

1 D.J. Moliterno, S.D.y Kristensen, R. De Caterina (Eds), Therapeutic Advances in Thrombosis, 2nd Edition, Wiley-Blackwell, Oxford 2012.

2 C. Becattini, M.C. Vedovati, G. Agnelli, *Thromb. Res.* 2012, **129**, 392–400.

3 M. Beinema, J.R.B.J. Brouwers, T. Schalekamp, B. Wilffert, *Thromb. Haemost.* 2008, **100**, 1052–1057.

4 A. G.G. Turpie, *Arterioscler. Thromb. Vasc. Biol*. 2007, **27**, 1238–1247.

5 P. L. Gross, J. I. Weitz, *Arterioscler. Thromb. Vasc. Biol.* 2008, **28**, 380–386.

6 S. Haas, *J. Thromb. Thrombolysis* 2008, **25**, 52–60.

7 F.F. van Doormaal, H. R. Büller, S. Middeldorp, *Critical Reviews in Oncology/Hematology* 2008, **66**, 145–154.

8 U. R. Desai, *Med. Res. Rev.* 2004, **24,** 151–181.

9 D. Wardrop, D. Keeling, *British J. Haematol*. 2008, **141**, 757–763.

10 G. A. Donnan, H. M. Dewey, B. R. Chambers, *Lancet Neurol.* 2004, **3**, 305–308.

11 J. W. Little, *Oral Radiol* 2012, **113,** 575–580.

12 K. M. O'Dell, D. Igawa, J. Hsin, *Clin. Ther.* 2012, **34**, 894–901.

13 S. Mantha, K. Cabral, J. Ansell, *Clinical Pharmacol. Therapeutics* 2013, **93**, 68–77.

14 M. Franchini, M. Mannucci, *Eur. J. Int. Med.* 2012, **23**, 692–695.

15 E.J. Valente, W.F. Trager, L.J. Jensen, *Acta Cryst.* 1975, B**31**, 954–960.

16 Y. C. Martin, *J. Comput. Aided Mol. Des.* 2009, **23**, 693–704.

17 A.R. Sheth, V.G. Young Jr, D.J.W. Grant, *Acta Cryst.* 2002, E**58**, m197–m199.

18 H. Henschel, B.C.G. Karlsson, A.M. Rosengren, I.A. Nicholls, *J. Mol. Struct., Theochem* 2010, **958**, 7–9.

19 I. Kostova, M. Amalanathan, I.H. Joe, *Chem. Phys.* 2010, 88–102.

20 I.H. Joe, I. Kostova, C. Ravikumar, M. Amalanathan, S. C. Pînzaru, *J. Raman Spectrosc.* 2009, **40**, 1033–1038.

21 W.R. Porter, *J. Comput. Aided Mol. Des.* 2010, **24**, 553–573.

22 B.C.G. Karlsson, G.D. Olsson, R. Friedman, A.M. Rosengren, H. Henschel, I.A. Nicholls, *J. Phys. Chem. B.* 2013, in press

23 M. Remko, *J. Mol. Struct., Theochem* 2009, **916**, 76–85.

24 H.Q. Liu, W.-G. Zhang, Z.-Q. Cai, W.-R. Xua, X.-P. Shena, *Acta Cryst.* 2012, E**68**, o3385.

25 M. J. Frisch, G. W. Trucks, H. B. Schlegel, G. E. Scuseria, M. A. Robb, J. R. Cheeseman, G. Scalmani, V. Barone, B. Mennucci, G. A. Petersson, H. Nakatsuji, M. Caricato, X. Li, H. P. Hratchian, A. F. Izmaylov, J. Bloino, G. Zheng, J. L. Sonnenberg, M. Hada, M. Ehara, K. Toyota, R. Fukuda, J. Hasegawa, M. Ishida, T. Nakajima, Y. Honda, O. Kitao, H. Nakai, T. Vreven, J. A. Montgomery, Jr., J. E. Peralta, F. Ogliaro, M. Bearpark, J. J. Heyd, E. Brothers, K. N. Kudin, V. N. Staroverov, R. Kobayashi, J. Normand, K. Raghavachari, A. Rendell, J. C. Burant, S. S. Iyengar, J. Tomasi, M. Cossi, N. Rega, J. M. Millam, M. Klene, J. E. Knox, J. B. Cross, V. Bakken, C. Adamo, J. Jaramillo, R. Gomperts, R. E. Stratmann, O. Yazyev, A. J. Austin, R. Cammi, C. Pomelli, J. W. Ochterski, R. L. Martin, K. Morokuma, V. G. Zakrzewski, G. A. Voth, P. Salvador, J. J. Dannenberg, S. Dapprich, A. D. Daniels, Ö. Farkas, J. B. Foresman, J. V. Ortiz, J. Cioslowski, and D. J. Fox, Gaussian 09, Version 9.0, Gaussian Inc., Wallingford, CT, 2011.

26 A. D. Becke, *Phys. Rev.* 1988, **A38**, 3098–3100.

27 A. D. Becke, *J. Chem. Phys.* 1993, **98**, 5648–5652.

28 C. Lee, W. Yang, R. G. Parr, *Phys. Rev.* 1988, **B37**, 785–789.

29 W.J.Hehre, L.Radom, P.v.R. Schleyer and J.A.Pople, Ab Initio Molecular Orbital Theory, Wiley, New York 1986.

30 S. Miertuš E. Scrocco J. Tomasi, *Chem. Phys.* 1981, **55**, 117–129.

31 A. Klamt, G. Schűűman, *J. Chem. Soc., Perkin Trans. 2*, 1993, 799–805.

32 V. Barone, M. Cossi, *J. Phys. Chem. A* 1998, **102**, 1995–2001.

33 M. Cossi, N. Rega, G. Scalmani, V. Barone, *J. Comp. Chem.* 2003, **24**, 669–681.

34 I. V. Tetko, J. Gasteiger, R. Todeschini, A. Mauri, D. Livingstone, P. Ertl, V. A. Palyulin E. V. Radchenko, N. S. Zefirov, A. S. Makarenko, V. Y. Tanchuk, V. V. Prokopenko, *J. Comput. Aided Mol. Des.* 2005, **19**, 453–463.

35 I. V. Tetko, P. Bruneau, H.W. Mewes, D. C. Rohrer, G. I. Poda, *Drug Discov. Today* 2006, **11,** 700–706.

36 http://archemcalc.com/sparc/

37 S. Hilal, S.W. Karickhoff, L.A. Carreira, *Quant. Struc. Act. Rel.,* 1995**, 14***,* 348–355.

38 L.A. Carreira, S. Hilal, S.W. Karickhoff, "Estimation of Chemical Reactivity Parameters and Physical Properties of Organic Molecules Using SPARC" in *Theoretical and Computational Chemistry*, Quantitative Treatment of Solute/Solvent Interactions, P. Politzer, J.S. Murray (Eds.), Elsevier Publishers, 1994.

39 S. Hilal, S.W. Karickhoff, L.A. Carreira, *QSAR Comb. Sci.* 2003**, 22***,* 565–574.

40 P. Ertl, P. Selzer, in *Handbook of Chemoinformatics: From Data to Knowledge*, J. Gasteiger, Ed., Wiley-VCH, Weinheim. 2003, pp. 1336–1348.

41 P. Ertl, B. Rohde, P. Selzer, *J. Med. Chem.*2000, **43**, 3714–3717.

42 http://www.molinspiration.com.

43 R.S. Porter, W.T. Sawyer, D.T. Lowenthal, *Warfarin*. In W.E. Ewans, J.J. Schentag, W.J. Jusko (Eds) Applied Pharmacokinetics, 2nd edn. Applied Therapeutics, Spokane, 1985, 1057–1104.

44 J. Ghuman, P.A. Zunszain, I. Petitpas, A.A. Bhattacharya, M. Otagiri, S. Curry, *J. Mol. Biol.* 2005**, 353**, 38–52.

45 I. Petitpas, A.A. Bhattacharya,, S. Tw ine, M. East, S. Curry, *J. Mol. Biol.* 2001**, 276**, 22804–22809.

46 Protein Data Bank. http://www.rscb.org/pdb/ (accessed May 2012)

47 F.H. Allen, S.E. Harris, R. Taylor, *J. Comput. Aided Mol. Des*. 1996, **10**, 247–254.

48 C.C. Pye, T. Ziegler, *Theor. Chem. Acc*., 1999, **101**, 396–408.

49 A. Bondi, *J. Phys. Chem.* 1964, **68**, 441–451.

50 M.C. Nicklaus, S. Wang, J.S. Driscoll, G.W.A. Milne, *Bioorg. Med. Chem.* 1995, **3**, 411–428.

51 J. Liebeschuetz, J. Hennemann, T. Olsson, C.R. Groom, *J. Comput. Aided Mol. Des.* 2012, **26**, 169–183.

52 M. Remko, S. Šoralová, *J. Biol. Inorg. Chem.* 2012, **17**, 621–630.

53 D.J. Ellis, M.H. Usman, P.G. Milner, D.M. Canafax, M.D. Ezekowitz, *Circulation* 2009, **129**, 1029–1035.

54 S.S. Bowersox, D. Canafax, P. Druzgala, P. Milner, J.I. Weitz, *Thromb. Res.* 2010, **126**, e383–e388.

55 A. Choppin, I. Irwin, L. Lach, M.G. McDonald, A.E. Rettie, L. Shao, C. Becker, M.P Palme, X. Paliard, S. Bowersox, D.M. Dennis, P. Druzgala, *Br. J. Pharmacol.* 2009, **158**, 1536–1547.

56 D. Kikelj, *Patophysiol. Haemost. Thromb*. 2003/2004, **33**, 487–491.

57 A.C. Spyropoulos, *Thromb. Res*. 2008, **123**, S29–S35.

58 V. J. Stella, K.G. Mooney, J.D. Pipkin, *J. Pharm. Sci.* 1984, **73**, 946–948.

59 M. He, K.R. Korzekwa, J.P. Jones, A.E. Rettie, W.F. Trager, *Arch. Biochem. Biophys.* 1999, **372**, 16–28.

60 N. H. Hauel, H. Nar, H. Priepke, U. Ries, J.-M. Stassen, W. Wienen, *J. Med. Chem*. 2002, **45**, 1757–1766.

61 A. Malkia, L. Murtomaki, A. Urtti , K. Kontturi, *Eur. J. Pharm. Sci*. 2004, **23**, 13–47.

62 S.K. Bhal, K. Kassam, I.G. Peirson, G.M. Pearl, *Mol. Pharm*. 2007, **4**, 556–560.

63 I.V. Tetko, V.Y. Tanchuk, A.E.P. Villa, *J. Chem. Inf. Comput. Sci.* 2001, **41**, 1407–1421.

64 I.V. Tetko, V.Y. Tanchuk, T.N. Kasheva, A.E.P. Villa, *J. Chem. Inf. Comput. Sci*. 2001, *41*, 1488–1493.

65 K.V. Balakin N.P. Savchuk I.V. Tetko, *Curr. Med. Chem.* 2006, **13**, 223–241.

66 W.M. Meylan, P. H. Howard, *J. Pharm. Sci*. 1995, **84**, 83–92.

67 http://www.syrres.com/

68 R.X. Wang, Y. Fu, L.H. Lai, *J. Chem. Inf. Comput. Sci*. 1997, **37**, 615–621.

69 R. X. Wang, Y. Gao, L. H. Lai, *Drug Discov. Des.* 2000 , **19**, 47–66.

70 D.S. Wishart, C. Knox, A.Ch. Guo, S. Shrivastava, M. Hassanali, P. Stothard, Z. Chang J. Woolsey, *Nucleic Acids Research*, 2006, **34**, D668–D672.

71 A.G. Leach, E.A. Pilling, A.A. Rabow, S. Tomasi, N. Assad, N.J. Buurma, A. Ballard, S. Narduolo, *Med. Chem. Commun.* 2012, **3**, 528–540.

72 F. Dullweber, M.T. Stubbs, D. Musil, J. Stürzebecher, G. Klebe, *J. Mol. Biol.* 2001, **313**, 593–614.

73 N.H. Hauel, H. Nar, H. Priepke, U. Ries, J.-M. Stassen, W. Wienen, *J. Med. Chem*. 2002, **45,** 1757–1766.

74 L. Xing, R.C. Glen, *J. Chem. Inf. Comput. Sci.* 2002*,* **42**, 796–805.

75 A. Avdeef, Absorption and Drug Development: Solubility, Permeability, and Charge State, Second Edition, John Wiley & Sons, Inc. 2012.

76 Y.H. Zhao, M.H. Abraham, J. Lee, A. Hersey, Ch.N. Luscombe, G. Beck, B. Sherborne, I. Cooper, *Pharm. Res*. 2002, **19**, 1446–1457.

77 D. F. Veber, S. R. Johnson, H.Y. Cheng, B. R. Smith, K. W. Ward, K. D. Kapple, *J. Med. Chem.* 2002, **45**, 2615–2623.

78 H. H. F. Refsgaard, B. F. Jensen, P. B. Brockhoff, S. B. Padkjær, M. Guldbrandt, M. S. Christensen, *J. Med. Chem.* 2005, 48, 805–811.

79 I. Muegge, *Med. Res. Rev.* 2003, 23, 302–321.

80 C.A. Lipinski, F. Lombardo, B. W. Dominy, P. J. Feeney, *Adv. Drug Delivery Rev*. 1997, 23, 3–25.

81 J. Steffel, T.F. Lüscher, *Kardiovask. Medizin* 2008, **11**, 337–345.

Table 1. Optimized dihedral angles[a] of the warfarin species studied

Dihedral angle, degrees		B3LYP/6–311++G(d,p)			CPCM – B3LYP/6–311++G(d,p)		
				R(+)-Warfarin			
	BDB 1H9Z	Tautomer A	Tautomer B	Hemiketal C	Tautomer A	Tautomer B	Hemiketal
α[C(2)-C(3)-C(7)-C(8)]	106.6	58.09	90.72		53.68	87.99	
β[C(3)-C(7)-C(8)-C(9)]	–90.4	-98.03	-68.95	-50.51	-112.86	-57.97	-46.22
γ[C(3)-C(7)-C(10)-C(11)]	159.7	-72.60	-57.97		-72.31	-61.39	
δ[C(7)-C(10)-C(11)-O(12)]	–30.1	-8.80	-8.42		-8.66	-13.74	
ε[C(3)-C(4)-O(5)-H]		-30.42			-29.37		
ζ[O(1)-C(2)-O(6)-H]			178.43			-1.67	
				S(-)-Warfarin			
	BDB 1HA2	Tautomer A	Tautomer B	Hemiketal C	Tautomer A	Tautomer B	Hemiketal
α[C(2)-C(3)-C(7)-C(8)]	87.6	90.81	96.65		88.44	104.02	
β[C(3)-C(7)-C(8)-C(9)]	–79.0	-140.26	-114.19	22.09	-141.08	-93.69	19.46
γ[C(3)-C(7)-C(10)-C(11)]	–144.6	146.81	156.63		145.07	163.12	
δ[C(7)-C(10)-C(11)-O(12)]	–131.8	-18.00	-21.98		-18.86	-14.97	
ε[C(3)-C(4)-O(5)-H]		1.25			-1.58		
ζ[O(1)-C(2)-O(6)-H]			-0.79			-1.14	
				R(+)-Warfarin sodium			
		Tautomer A	Tautomer B		Tautomer A	Tautomer B	
α[C(2)-C(3)-C(7)-C(8)]		74.03	88.90		69.87	85.99	
β[C(3)-C(7)-C(8)-C(9)]		-83.39	-70.55		-98.98	-55.83	
γ[C(3)-C(7)-C(10)-C(11)]		-69.43	-60.63		-71.52	-65.15	
δ[C(7)-C(10)-C(11)-O(12)]		-24.48	-12.21		-18.45	-19.21	
ε[C(3)-C(4)-O(5)-Na]		-58.51			-68.04		
ζ[O(1)-C(2)-O(6)-Na]			0.50			-1.78	
				S(-)-Warfarin sodium			
		Tautomer A	Tautomer B		Tautomer A	Tautomer B	
α[C(2)-C(3)-C(7)-C(8)]		136.21	95.23		119.05	101.31	
β[C(3)-C(7)-C(8)-C(9)]		134.45	-116.11		118.63	-99.88	
γ[C(3)-C(7)-C(10)-C(11)]		154.89	157.41		167.70	162.51	
δ[C(7)-C(10)-C(11)-O(12)]		104.76	-22.56		139.24	-15.51	
ε[C(3)-C(4)-O(5)-Na]		50.04			95.17		
ζ[O(1)-C(2)-O(6)-Na]			2.85			1.23	

Table 2 Optimized dihedral angles[a] of the coumarinic anticoagulants studied

Dihedral angle, degrees	B3LYP/6–311++G(d,p)		CPCM – B3LYP/6–311++G(d,p)	
		R(+)-Acenocoumarol		
	Tautomer A	Tautomer B	Tautomer A	Tautomer B
α[C(2)-C(3)-C(7)-C(8)]	57.37	88.54	53.40	87.54
β[C(3)-C(7)-C(8)-C(9)]	-100.51	-75.67	-114.57	-60.84
γ[C(3)-C(7)-C(10)-C(11)]	-73.37	-60.36	-73.01	-62.87
δ[C(7)-C(10)-C(11)-O(12)]	-8.27	-7.54	-8.64	-14.46
ε[C(3)-C(4)-O(5)-H]	-30.62		-29.13	
ζ[O(1)-C(2)-O(6)-H]		-0.92		-1.94
		S(-)- Acenocoumarol		
	Tautomer A	Tautomer B	Tautomer A	Tautomer B
α[C(2)-C(3)-C(7)-C(8)]	88.51	97.13	86.96	106.44
β[C(3)-C(7)-C(8)-C(9)]	-137.45	-114.50	-139.26	-90.88
γ[C(3)-C(7)-C(10)-C(11)]	148.63	158.81	146.78	165.34
δ[C(7)-C(10)-C(11)-O(12)]	-14.83	-16.96	-16.39	-11.02
ε[C(3)-C(4)-O(5)-H]	-2.00		-3.86	
ζ[O(1)-C(2)-O(6)-H]		-0.80		-0.81
		R(+)-Phenprocoumon		
	Tautomer A	Tautomer B	Tautomer A	Tautomer B
α[C(2)-C(3)-C(7)-C(8)]	122.94	93.45	121.26	97.05
β[C(3)-C(7)-C(8)-C(9)]	-42.96	-44.80	-41.03	-39.07
γ[C(3)-C(7)-C(10)-C(11)]	83.89	99.79	84.78	99.16
δ[C(7)-C(10)-C(11)-O(12)]				
ε[C(3)-C(4)-O(5)-H]	15.85		12.22	
ζ[O(1)-C(2)-O(6)-H]		-2.71		-1.65
		S(-)-Phenprocoumon		
	Tautomer A	Tautomer B	Tautomer A	Tautomer B
α[C(2)-C(3)-C(7)-C(8)]	-141.70	-100.70	-140.94	-101.08
β[C(3)-C(7)-C(8)-C(9)]	70.03	107.31	70.07	106.13
γ[C(3)-C(7)-C(10)-C(11)]	-162.78	-167.67	-162.68	-166.72
δ[C(7)-C(10)-C(11)-O(12)]				
ε[C(3)-C(4)-O(5)-H]	-10.22		-8.69	
ζ[O(1)-C(2)-O(6)-H]		0.04		1.16

[a]For definition of dihedral angles see Fig. 1.

Table 2 – Continued

Dihedral angle, degrees	B3LYP/6–311++G(d,p)		CPCM B3LYP/6–311++G(d,p)	
	Tecarfarin			
	Tautomer A	Tautomer B	Tautomer A	Tautomer B
α[C(2)-C(3)-C(7)-C(8)]	126.28	91.32	117.33	84.72
β[C(3)-C(7)-C(8)-C(9)]	-53.15	-98.60	-41.57	-115.17
ε[C(3)-C(4)-O(5)-H]	10.85		4.24	
ζ[O(1)-C(2)-O(6)-H]		-0.84		-1.13
	Tecarfarin sodium			
	Tautomer A	Tautomer B	Tautomer A	Tautomer B
α[C(2)-C(3)-C(7)-C(8)]	124.76	88.86	95.78	80.78
β[C(3)-C(7)-C(8)-C(9)]	-40.91	-98.72	-5.89	-142.77
ε[C(3)-C(4)-O(5)-Na]	49.39		18.32	
ζ[O(1)-C(2)-O(6)-Na]		2.55		-3.43

Table 3 – Optimized dihedral angles[a] of the direct thrombin inhibitors studied

Dihedral angle, degrees	X-ray		B3LYP/6–31++g(p,d)[d]	B3LYP/6–311++g(p,d)	CPCM B3LYP/6–311++g(p,d)
	pdb.4BAH	pdb.1K1P		Melagatran	
α[C(1)-C(2)-N(3)-C(5)]	-166.50	-171.06		170.15	173.48
β[C(2)-N(3)-C(5)-C(6)]	60.74	63.69		-72.13	-71.65
γ[C(2)-N(3)-C(5)-C(4)]	179.89	-172.11		164.42	163.95
δ[N(3)-C(5)-C(6)-N(7)]	-137.49	-158.34		158.57	154.02
ε[N(7)-C(8)-C(9)-N(10)]	127.48	125.33		56.94	46.59
ζ[C(9)-N(10)-C(11)-C(12)]	117.55	114.07		107.56	116.52
η[N(10)-C(11)-C(12)-C(13)]	81.68	106.58		112.92	123.03
θ[C(14)-C(15)-C(16)]-N(17)]	158.73	149.89		155.52	150.84
				Ximelagatran	
α[C(1)-C(2)-N(3)-C(5)]				172.05	172.18
β[C(2)-N(3)-C(5)-C(6)]				-70.77	-72.42
γ[C(2)-N(3)-C(5)-C(4)]				164.30	162.94
δ[N(3)-C(5)-C(6)-N(7)]				157.28	155.30
ε[N(7)-C(8)-C(9)-N(10)]				56.77	47.55
ζ[C(9)-N(10)-C(11)-C(12)]				110.20	120.14
η[N(10)-C(11)-C(12)-C(13)]				105.84	127.47
θ[C(14)-C(15)-C(16)]-N(17)]				151.83	148.70
	pdb.1KTS[b]			Dabigatran	
α[C(1)-C(2)-N(3)-C(4)]	83.0		144.7	145.59	139.59
β[C(2)-N(3)-C(4)-O(5)]	-170.8		152.7	152.26	155.95
γ[C(2)-N(3)-C(4)-C(6)]	4.5		-32.6	-32.88	-28.32
δ[N(3)-C(4)-C(6)-C(7)]	-132.6		-34.2	-35.28	-40.50
ε[N(8)-C(9)-C(10)-N(11)]	-31.1		-125.7	-125.12	-119.74
ζ[C(9)-C(10)-N(11)-C(12)]	79.3		78.1	78.65	81.01
η[C(10)-N(11)-C(12)-C(13)]	33.3		-16.3	-16.40	-14.18
θ[C(14)-C(15)-C(16)]-N(17)]	-176.7		158.1	157.58	154.59
	X-ray[c]			Dabigatran etexilate	
α[C(1)-C(2)-N(3)-C(4)]	88.2		145.5	146.03	139.52
β[C(2)-N(3)-C(4)-O(5)]	0.6		153.5	153.19	155.65
γ[C(2)-N(3)-C(4)-C(6)]	177.9		-31.6	-31.77	-28.50
δ[N(3)-C(4)-C(6)-C(7)]	134.4		-35.0	-35.85	-40.48
ε[N(8)-C(9)-C(10)-N(11)]	-1.5		-122.9	-122.34	-119.86
ζ[C(9)-C(10)-N(11)-C(12)]	-176.6		79.6	80.03	79.05
η[C(10)-N(11)-C(12)-C(13)]	-5.8		-16.9	-16.86	-10.87
θ[C(14)-C(15)-C(16)]-N(17)]	–175.9		160.7	160.15	157.96

[a]For definition of dihedral angles see Fig. 1.
[b]Dabigatran ethylester
[c]Reference 24
[d]Reference 23

Table 4. Relative stability of individual tautomers and enantiomers of the coumarinic anticoagulants

Compound	Tautomer	E_{tot}, a.u.	E^{CPCM}_{tot}, a.u.	ΔE, kJ/mol	ΔE^{CPCM}, kJ/mol
R(+)-Warfarin	A	–1034.858 303	–1034.873 945	0	0
	B	–1034.836 362	–1034.856 714	57.61	45.24
	C (Hemiketal)	–1034.854 952	–1034.872 840	8.79	2.90
S(–)-Warfarin	A	–1034.844 272	–1034.864 265	36.84	25.41
	B	–1034.838 885	–1034.856 549	50.98	45.67
	C (Hemiketal)	–1034.852 845	–1034.871 379	14.32	6.73
R(+)-Warfarin sodium	A	–1196.625 365	–1196.677 021	0	0
	B	–1196.597 124	–1196.671 635	74.14	14.14
S(–)-Warfarin sodium	A	–1196.614 036	–1196.671 205	29.74	15.26
	B	–1196.600 085	–1196.670 957	66.37	15.92
R(+)-Acenocoumarol	A	–1239.422 760	–1239.443 687	0	0
	B	–1239.401 673	–1239.426 576	55.36	44.92
S(–)-Acenocoumarol	A	–1239.408 054	-1239.433 305	38.31	27.23
	B	–1239.404 866	–1239.427 012	46.98	43.78
R(+)-Phenprocoumon	A	–921.481 935	–921.493 512	22.19	22.99
	B	–921.468 225	–921.482 789	58.18	51.14
S(–)-Phenprocoumon	A	–921.490 387	–921.502 269	0	0
	B	–921.475 918	–921.488 406	37.98	36.39
Tecarfarin	A	–1784.395 386	–1784.412 223	0	0
	B	–1784.384 729	–1784.401 271	27.97	28.75
Tecarfarin sodium	A	–1946.154 011	–1946.218 550	0	0
	B	–1946.147 321	–1946.216 957	17.56	4.18

Table 5

The CPCM B3LYP/6–311++G(d,p) calculated solvation free energies ΔG^{CPCM} (kJ/mol) of the anticoagulant agents investigated[a]

Drug	Tautomer	ΔG^{CPCM}	Gas-phase dipole moment, Debye (D)
R(+)-Warfarin	A	–41.06	2.20
	B	–53.43	5.28
	C (Hemiketal)	–46.96	5.75
S(–)-Warfarin	A	–52.49	6.25
	B	–46.37	4.84
	C (Hemiketal)	–48.66	6.05
R(+)-Warfarin sodium	A	–135.62	9.05
	B	–195.63	13.29
S(–)-Warfarin sodium	A	–150.09	9.65
	B	–186.07	12.01
R(+)-Acenocoumarol	A	–54.94	7.44
	B	–65.38	8.19
S(–)-Acenocoumarol	A	–66.29	8.94
	B	–58.14	9.59
R(+)-Phenprocoumon	A	–30.39	4.08
	B	–38.23	4.79
S(–)-Phenprocoumon	A	–31.19	4.17
	B	–32.78	4.89
Tecarfarin	A	–44.21	4.40
	B	–43.43	8.09
Tecarfarin sodium	A	–169.44	9.99
	B	–182.83	15.63
Melagatran		–80.42	4.51
Ximelagatran		–73.11	5.16
Dabigatran		–101.67	5.05
Dabigatran etaxilate		–104.58	7.06

[a] Water as solvent

Table 6. The pK_a values (acidities) of the anticoagulants investigated (SPARC/pK_a)

	p*K*a[a],		% Ionized form	
	Acid function	Basic function	Acid function	Basic function
Acenocoumarol A	5.40		99.0	
Acenocoumarol B	4.96		99.6	
Phenprocoumon A	5.96		96.5	
Phenprocoumon B	5.52		98.7	
Warfarin A	5.67		98.1	
Warfarin B	5.23		99.3	
Warfarin C (Hemiketal)	17.75		0	
Tecarfarin A	5.73		97.9	
Tecarfarin B	5.95		96.5	
Melagatran	4.12	11.00	100	100
Dabigatran	4.24	11.51	100	100

Table 7. Calculated lipophilicity and solubility of the anticoagulants studied

Drug	LogP[a], exp	ALOGPS	KoWWIN	XLOGP3	LogD, (pH=7.4)	Solubility[a] (exp.)	ALOGPS
Acenocoumarol A		2.53	2.85	2.53	0.52		-4.52 (10.65 mg/L)
Acenocoumarol B	1.98	2.55	2.28	2.53	0.11		-4.53 (10.47 mg/L)
Phenprocoumon A		3.81	3.79	3.62	2.35		-3.76 (48.65 mg/L)
Phenprocoumon B	3.62	3.70	4.02	3.62	1.81	12.9 mg/L	-3.77 (47.24 mg/L)
Warfarin A		2.41	2.23	2.70	0.67		-3.82 (47.17 mg/L)
Warfarin B	2.70	2.55	2.46	2.70	0.38	17 mg/L	-3.81 (47.72 mg/L)
Warfarin C (Hemiketal)		3.14	2.98	3.12			-3.63 (72.21 mg/L)
Tecarfarin_A		4.14	3.58	4.85	2.46		-4.98 (4.81 mg/L)
Tecarfarin_B		4.44	5.14	5.66	2.97		-5.24 (2.65 mg/L)
Melagatran		-0.51	-1.93	-0.99	-3.79		-3.57 (0.12 g/L)
Ximelagatran		1.35	0.58	2.16			-3.75 (84.54 mg/L)
Dabigatran		2.37	1.95	1.70	-0.79		-3.68 (97.47 mg/L)
Dabigatran Etexilate	3.8	5.17	5.58	5.65		1.8 mg/mL	-5.13 (4.66 mg/L)

[a]Drug file DrugBank[70]

Table 8

Calculated absorption (%ABS), polar surface area (PSA) and Lipinski parameters of the anticoagulants studied

Drug	%ABS	Volume	PSA	NROTB	*n* ON acceptors	*n* OHNH donors	Formula weight
Acenocoumarol	69.9	300.52	113.34	5	7	1	353.33
Phenprocoumon	91.6	258.21	50.44	3	3	1	280.32
Warfarin	85.7	277.18	67.51	4	4	1	308.33
Warfarin (Hemiketal)	88.4	272.85	59.67	1	4	1	308.33
Tecarfarin	82.5	348.44	76.74	7	5	1	460.33
Melagatran	57.7	400.21	148.61	9	9	6 (viol.)	429.52
Ximelagatran	58.5	443.51	146.35	11	10	5	473.52
Dabigatran	57.2	419.63	150.22	9	10	5	471.52
Dabigatran Etexilate	55.9	583.46	154.05	17	12 (viol.)	3	627.75 (viol.)

Figure Captions

Fig. 1. Structure and atom labeling in the anticoagulant drugs studied

Fig. 2.

(A) - Molecular superimposition of the Becke3LYP optimized molecular structure of *R*(+)-warfarin (red) and *R*(+)-warfarin from the cocrystal with human serum albumin myristate, PDB 1H9Z (green).

(B) - Molecular superimposition of the Becke3LYP optimized molecular structure of *S*(–)-warfarin (red) and *S*(–)-warfarin from the cocrystal with human serum albumin myristate, PDB 1HA2 (green).

Fig. 3.

Molecular superimposition of the Becke3LYP optimized molecular structure of *R*(+)-phenprocoumon (blue) and *S*(–)-phenprocoumon (green).

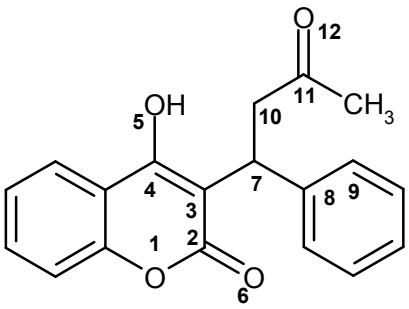

Warfarin, tautomer A

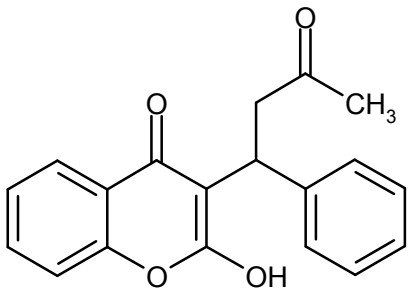

Warfarin, tautomer B

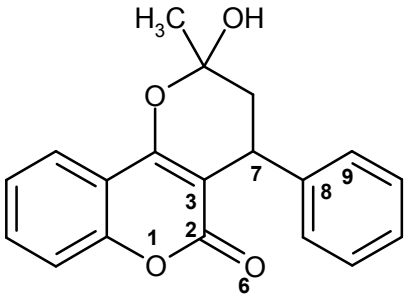

Warfarin, tautomer C (hemiketal)

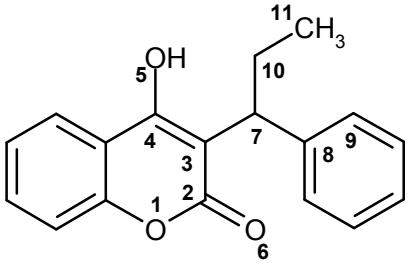

Phenprocoumon, tautomer A

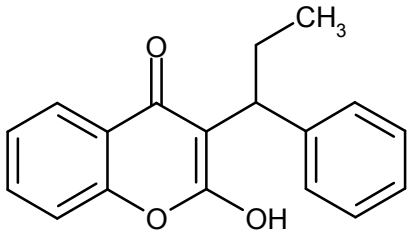

Phenprocoumon, tautomer B

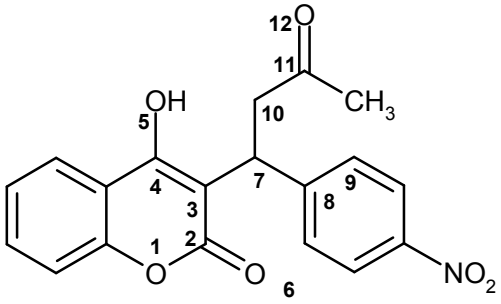

Acenocoumarol, tautomer A

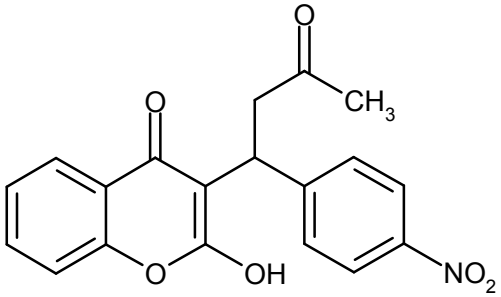

Acenocoumarol, tautomer B

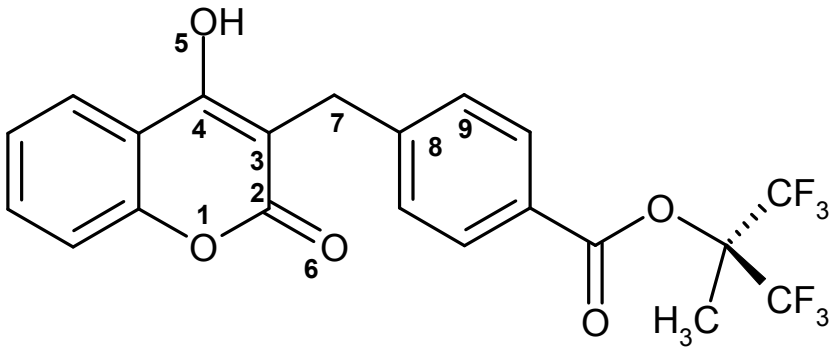

Tecarfarin, tautomer A

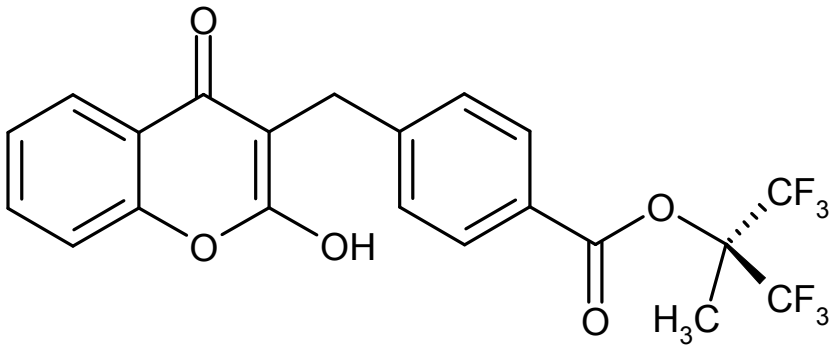

Tecarfarin, tautomer B

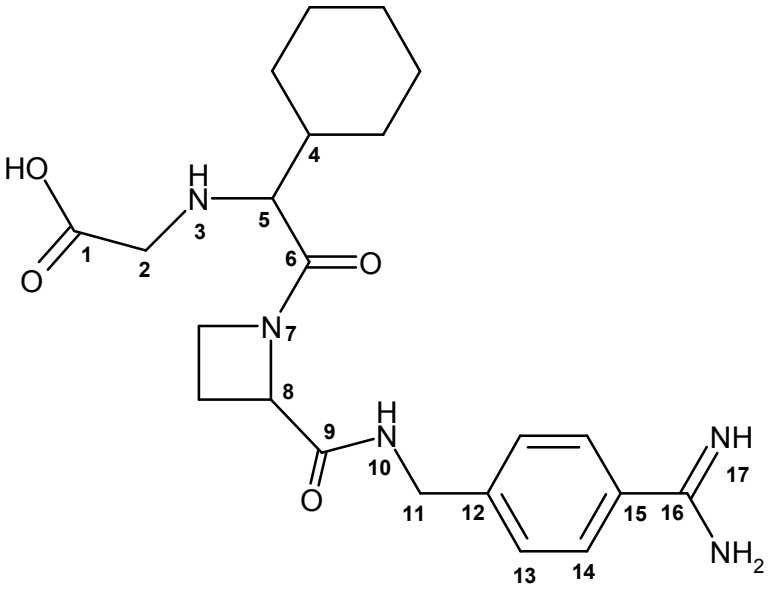

Melagatran

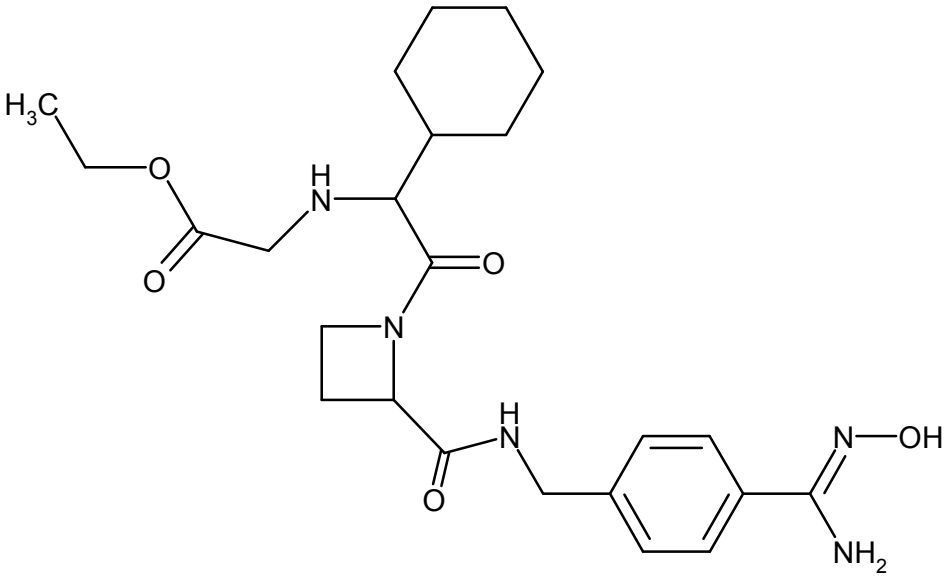

Ximelagatran

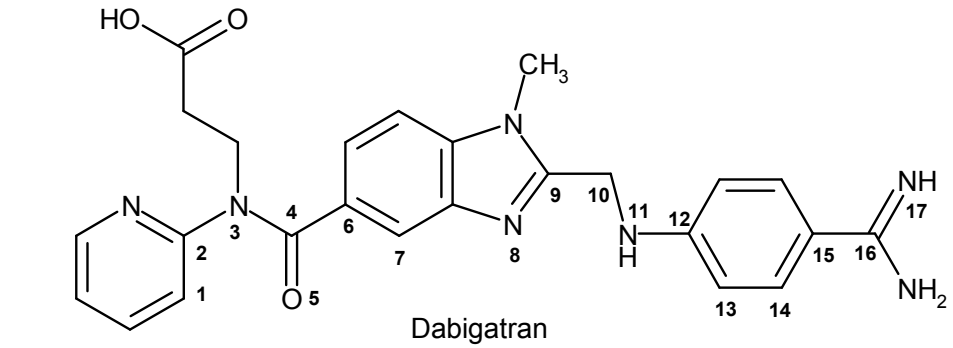

Dabigatran

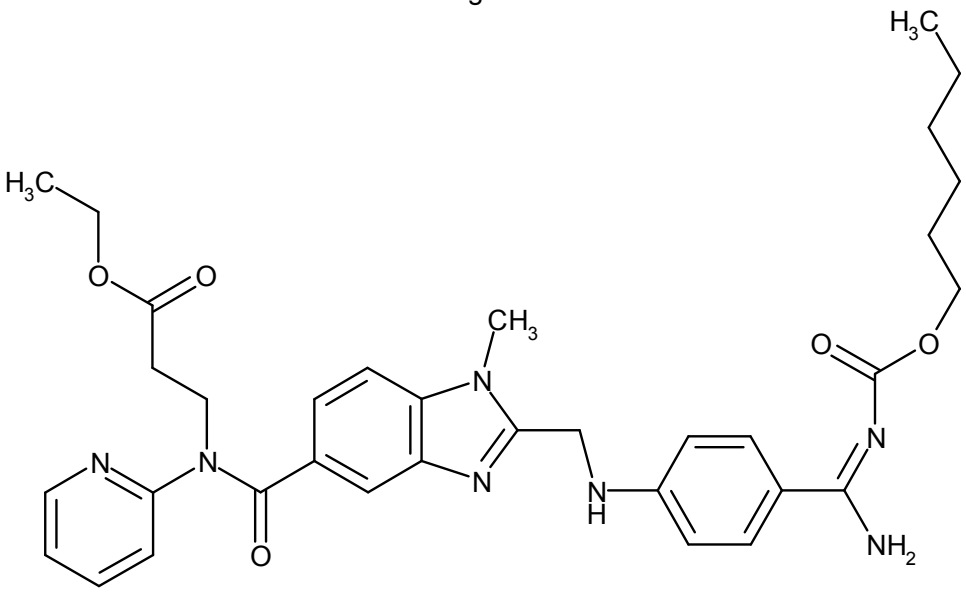

Dabigatran Etexilate

Fig. 1

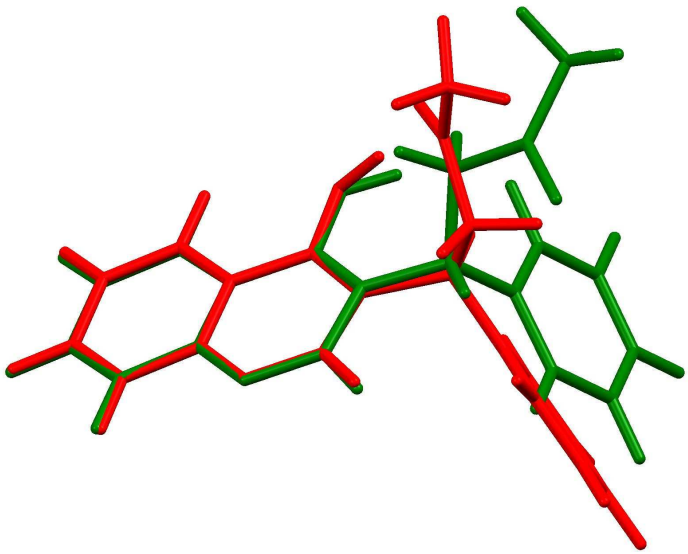

A

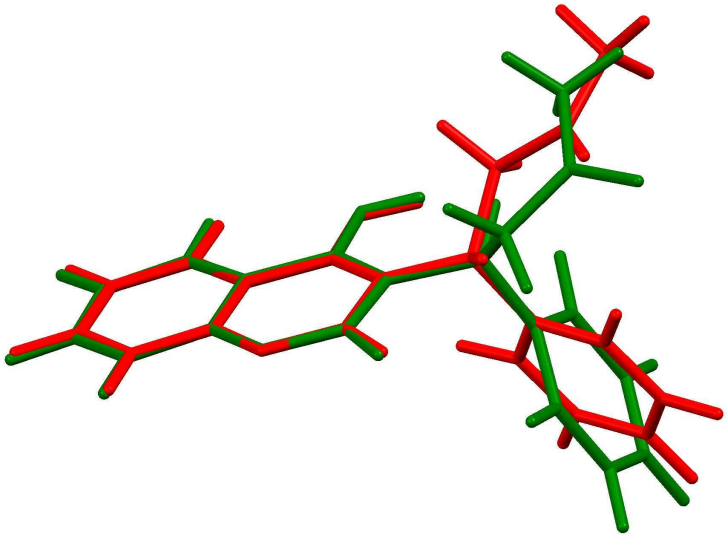

B

Fig. 2

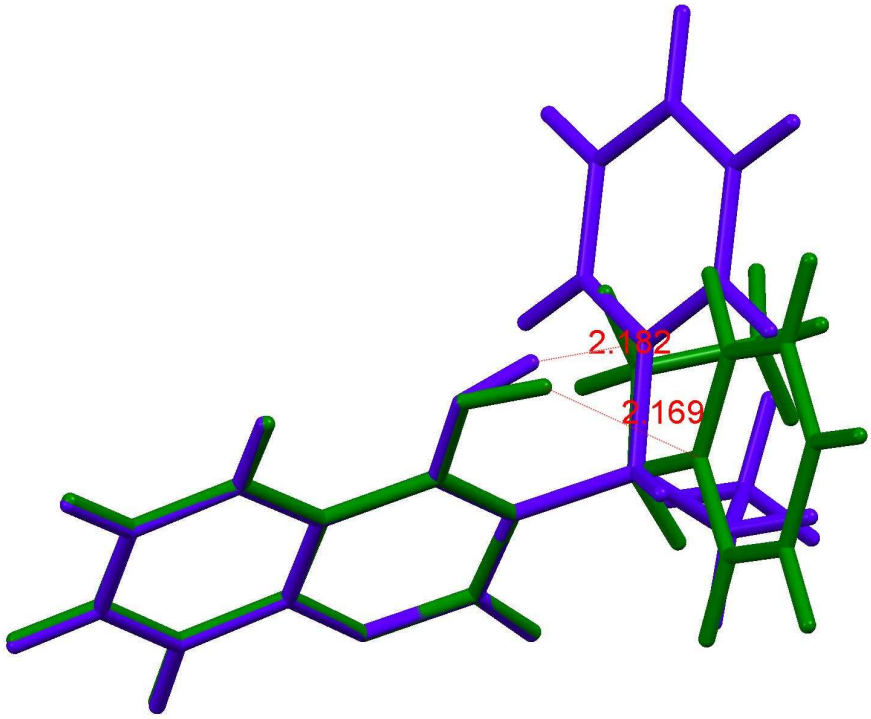

Fig. 3